Iron-phthalocyanine molecular junction with high spin filter efficiency and negative differential resistance

Huang, Jing; Xu, Ke; Lei, Shulai; Su, Haibin; Yang, Shangfeng; Li, Qunxiang; Yang, Jinlong

2012

Huang, J., Xu, K., Lei, S., Su, H., Yang, S., Li, Q., et al. (2012). Iron-phthalocyanine molecular junction with high spin filter efficiency and negative differential resistance. The Journal of Chemical Physics, 136(6), 064707.

https://hdl.handle.net/10356/95241

https://doi.org/10.1063/1.3684551

Iron-phthalocyanine molecular junction with high spin filter efficiency and negative differential resistance

Jing Huang, Ke Xu, Shulai Lei, Haibin Su, Shangfeng Yang et al.

Citation: J. Chem. Phys. **136**, 064707 (2012); doi: 10.1063/1.3684551
View online: http://dx.doi.org/10.1063/1.3684551
View Table of Contents: http://jcp.aip.org/resource/1/JCPSA6/v136/i6
Published by the American Institute of Physics.

Iron-phthalocyanine molecular junction with high spin filter efficiency and negative differential resistance

Jing Huang,[1,2] Ke Xu,[2] Shulai Lei,[2] Haibin Su,[3] Shangfeng Yang,[2] Qunxiang Li,[2,a)] and Jinlong Yang[2]

[1]*School of Materials and Chemical Engineering, Anhui University of Architecture, Hefei, Anhui 230022, People's Republic of China*
[2]*Hefei National Laboratory for Physical Sciences at Microscale, University of Science and Technology of China, Hefei, Anhui 230026, People's Republic of China*
[3]*Division of Materials Science, Nanyang Technological University, 50 Nanyang Avenue, 639798, Singapore*

(Received 25 October 2011; accepted 17 January 2012; published online 13 February 2012)

We investigate the spin transport properties of iron-phthalocyanine (FePc) molecule sandwiched between two N-doped graphene nanoribbons (GNRs) based on the density functional theory and nonequilibrium Green's function methods. Our calculated results clearly reveal that the FePc molecular junction has high spin-filter efficiency as well as negative differential resistance (NDR). The zero-bias conductance through FePc molecule is dominated by the spin-down electrons, and the observed NDR originates from the bias-dependent effective coupling between the FePc molecular orbitals and the narrow density of states of electrodes. The remarkable high spin-filter efficiency and NDR are robust regardless of the edge shape and the width of GNRs, and the N-doping site in GNRs. These predictions indicate that FePc junction holds great promise in molecular electronics and spintronics applications. © *2012 American Institute of Physics*. [http://dx.doi.org/10.1063/1.3684551]

I. INTRODUCTION

Molecular spintronics, in which molecules are used as spin transport channels, has attracted enormous research attentions since it holds promise for the next generation of electronic devices with enhanced functionality and improved performance.[1–4] In the past years, much research has focused on metal phthalocyanines (MPcs),[5–9] Fe_4 derivatives,[10] Mn_{12} magnet,[11] and magnetic organometallic molecular wires.[12–16] Among them, MPcs form a promising family of compounds due to their tunable electronic and magnetic properties by changing the central transition metal atom. In the past years, the adsorption behaviors of MPcs on various substrates have been extensively investigated.[5–7,17] A few studies have been reported on the electronic transport properties of MPc molecules sandwiched between the low-dimensional electrodes.[8,9,18,19] For example, Tomofuni *et al.* calculated the electronic transmission of CuPc molecule sandwiched between gold cluster electrodes,[18] and found that the symmetry-matched interaction between CuPc and the gold cluster electrodes is important to enhance the transmission function. Calzolari *et al.* examined the electronic correlation's influence on the transport property through CuPc and MnPc molecules connected to gold chain electrodes with sulfur atoms.[19] Shen *et al.* investigated the spin transport properties of MPcs (M = Mn, Fe, Co, Ni, Cu, and Zn) sandwiched between two semi-infinite (4,4) armchair single-walled carbon nanotubes and found that only MnPc and FePc can act as nearly perfect spin filters.[8,9]

Enabled by the unique physical properties of graphene nanoribbons (GNRs) (Refs. 20–22) and the successful fabrication of GNRs with various widths using the mechanical method or a chemical route,[23,24] GNRs have been recently employed as the electrodes for several molecular devices, including molecular switch,[25] negative differential resistance (NDR),[26,27] and spin filter.[28,29] Motivated by a recent preliminary experiment that CuPc thin film within the graphene nanogap electrodes displays high transistor performance,[24] we examine the spin transport properties of FePc molecule sandwiched between two N-doped GNR electrodes[27] by employing the non-equilibrium Green's function formalism combined with spin density functional theory. The calculated results clearly demonstrate that the spin-resolved zero-bias conductance through the proposed FePc molecular junction is dominated by the spin-down electrons with high spin-filter efficiency (SFE). At the same time, it exhibits NDR, originating from the bias-dependent coupling between the discrete frontier molecular orbitals (MOs) in the scattering region and the density of states of N-doped GNR electrodes. Moreover, the dual-function in the proposed FePc molecular junctions, namely, the high SFE and NDR, is robust regardless of the edge shape of GNR electrodes.

II. COMPUTATIONAL MODEL AND METHOD

Our proposed molecular junction is a two-probe system, in which an FePc molecule is sandwiched between N-doped GNR electrodes. Figure 1 shows an FePc molecular junction. Here, two N-doped armchair GNRs (AGNRs) with width W = 13 (named as 13-AGNRs) are modeled with a supercell (10 Å × 30 Å × 8.53 Å). The N-dopant, labeled with "N" with a blue ball in Fig. 1, locates at the center of 13-AGNRs, and a 10 Å vacuum slab is used to eliminate interaction between AGNRs in neighboring cells. The examined molecular

a) Author to whom correspondence should be addressed. Electronic mail: liqun@ustc.edu.cn.

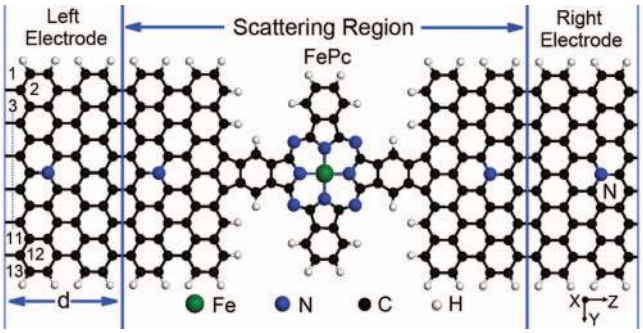

FIG. 1. The optimized two-probe geometry of an FePc molecule sandwiched between two N-doped AGNR electrodes. Here, the label "N" stands for the doping site, the blue vertical lines denote the scattering region, and d (about 8.53 Å) stands for the optimized lattice constant of N-doped AGNR electrodes.

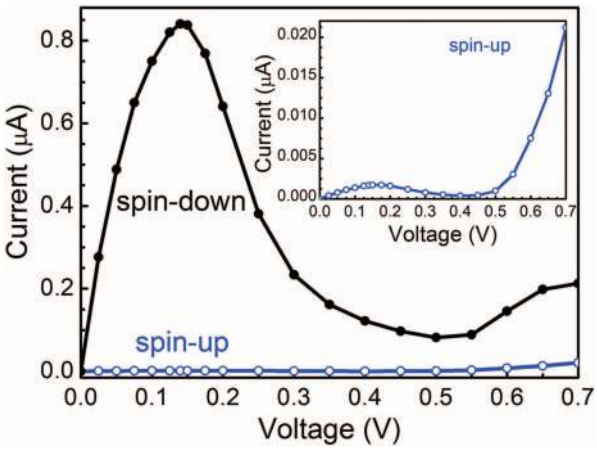

FIG. 2. The calculated spin-resolved I-V curves of FePc molecular junction. The black and blue lines stand for the current of spin-down and spin-up electrons, respectively. For clarity, the right above inset is the I-V curve for the spin-up electrons in smaller scale.

junction can be divided into three parts: scattering region, left electrode, and right electrode. All edge carbon atoms are saturated with hydrogen atoms. The geometric and electronic properties are calculated by using the spin-polarized density functional theory (DFT) method implemented in the Spanish Initiative for Electronic Simulations with Thousands of Atoms (SIESTA) package.[30] The generalized gradient approximation (GGA) in the Perdew-Burke-Ernzerhof form (PBE) (Ref. 31) is used to describe the exchange and correlation energy. The core electrons are modeled with Troullier-Martins nonlocal pseudopotential, and the valence electrons are expanded over a finite range numerical basis set. Double-zeta polarized basis are used for all elements including carbon, nitrogen, hydrogen, and iron atoms. The cutoff energy is 150 Ry and a Monkhorst-Pack K-mesh of $1 \times 1 \times 200$ is used. All atomic positions are fully relaxed until the force tolerance to 0.01 eV/Å. Note that the numerical integration in the complex plane of G-lesser Green's function implemented in ATK works well for noble metal electrodes since their density of states is a smooth function of single-particle energy.[34] If using graphene as electrodes in molecular junction, one should carefully manage them since their density of states is very irregular with many narrow resonances. We used 60 contour points, with a lower energy bound of 3 Ry (1 Ry = 13.6 eV) in the contour diagram in the case of zero bias and additional contour points spaced at 0.01 eV along the real energy axis in the case of nonzero bias voltage.

The spin transport properties through FePc molecule are studied with DFT calculations combined with nonequilibrium Green's function technique implemented in the ATK package,[32,33] which has successfully addressed many experimental results.[34] The spin-polarized current-voltage (I-V) curves are obtained by using the Landauer-Büttiker formula as

$$I(V) = \frac{e}{h}\int T_\sigma(E, V)[f(E-\mu_L) - f(E-\mu_R)]dE, \quad (1)$$

here, $T_\sigma(E, V)$ is transmission functions for the spin-up and spin-down electrons ($\sigma = \uparrow/\downarrow$), defined as $T_\sigma(E, V) = Tr[\Gamma_L G_\sigma \Gamma_R G_\sigma^+]$, G_σ is the spin-dependent retarded Green's function of the extended molecule, $\Gamma_{L/R}$ is the coupling matrix between the scattering region and the left/right electrode, $f(E-\mu_{L(R)})$ is the Fermi function, and $\mu_{L/R}$ stands for the chemical potential of left/right electrode, respectively.

III. RESULTS AND DISCUSSION

Figure 2 shows the spin-polarized I-V curves of FePc molecule sandwiched between two N-doped 13-AGNRs in the bias voltage range from 0.0 to 0.7 V. At each bias, the current is determined self-consistently under the nonequilibrium condition. As seen in Fig. 2, the calculated I-V curves clearly demonstrate two following important features: (i) The current of the spin-down electrons ($I_\downarrow$) through the molecular junction is remarkably larger that of the spin-up electrons ($I_\uparrow$). For example, the calculated current at 0.14 V is about 1.7×10^{-3} and 0.84 μA for the spin-up and spin-down electrons, respectively. The remarkable difference of current between the spin-up and spin-down electrons under the applied bias can be quantified by the ratio of the current defined as $R(V) = I_\downarrow(V_{bias})/I_\uparrow(V_{bias})$. The calculated R(V) varies from around 80 to 500 in the examined bias window. Such a large ratio can be readily measured for the real applications with the FePc molecule junction. (ii) The current of the spin-down electrons initially increases with the applied V_{bias}, and clearly presents a NDR character between 0.14 and 0.5 V for the spin-down electrons. The maximum current of the spin-down electrons is up to be about 0.84 μA at the peak position (V_{bias} = 0.14 V), while the current reaches its minimum value (0.08 μA) at the valley site (V_{bias} = 0.5 V). Actually, NDR also appears in the bias range of 0.15–0.4 V for the spin-up electrons, as shown in the inset of Fig. 2. It turns high peak-to-valley ratios of NDR for two spin channels. The ratio is about 5 and 10 for spin-up and spin-down electrons, respectively. The NDR of the FePc junction highlights its promising potential for electronic amplifiers, logic gates, and fast switch devices.[2,7]

These observations imply that significant spin filter effect and obvious NDR can coexist remarkably in the proposed FePc molecular junction, which, to the best of our

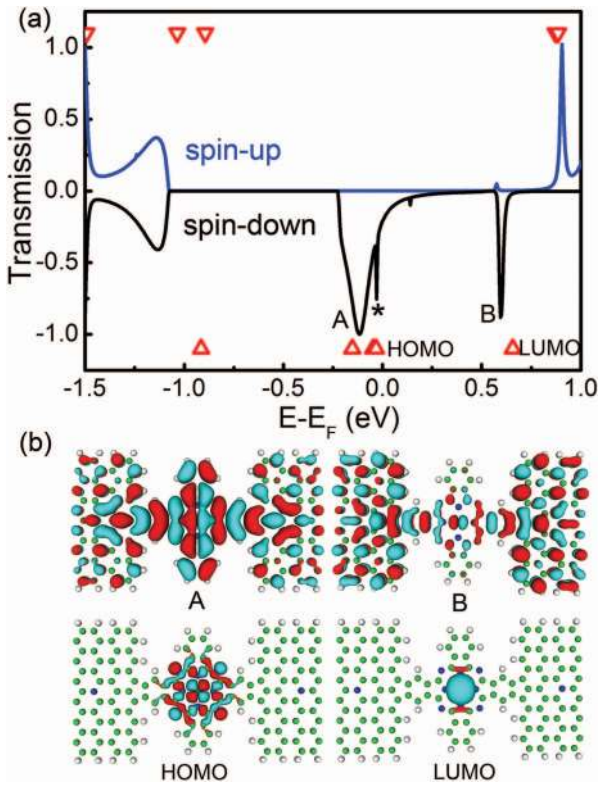

FIG. 3. (a) The energy dependent spin-resolved transmission spectra of FePc molecular junction. The blue and black curves stand for the transmission of the spin-up and spin-down electrons, respectively. Empty triangles denote the molecular projected self-consistent Hamiltonian eigenvalues. (b) Contour plots of eigenfunctions. Here, the top panel stands for two eigenfunctions of the scattering region, which contribute the transmission peaks A and B. The perturbed HOMO and LUMO of the FePc molecular projected self-consistent Hamiltonian in the scattering region are illustrated in the bottom panel.

knowledge, has not been reported in all the studies on the FePc molecular junctions so far,[9] though this dual function has been reported recently in organometallic Fe–C_5H_5 and Fe–$C_5(CH_3)_5$ nanowires.[14,16] Clearly, both spin filter effect and NDR are desirable features with ample applications in future molecular electronics and spintronics.

To understand the nature of the observed spin filter effect, we plot the spin-polarized zero-bias transmission spectra of the proposed FePc molecular junction with N-doped 13-AGNR electrodes in Fig. 3(a). It is clear that the transmission spectra of the spin-up and spin-down electrons through FePc molecule display remarkably different behavior around the Fermi level. For the spin-down electrons, two significant transmission peaks, labeled with **A** and **B** in Fig. 3(a), representing the conductance channels through the molecular junction, are located at −0.11 and 0.6 eV, respectively. Meanwhile, the transmission coefficient of the spin-up channel is quite small in the wide energy region from −1.05 to 0.85 eV. The distinct difference of transmission spectrum between two spin channels can be evaluated with spin filter efficiency (SFE) at the Fermi level, defined as SFE = $[T_\uparrow(E_F) - T_\downarrow(E_F)]/[T_\uparrow(E_F) + T_\downarrow(E_F)]$. Here, $T_\uparrow$ and $T_\downarrow$ stand for the transmission coefficient of the spin-up and spin-down electrons, respectively. The positive SFE denotes a conductance dominated by the spin-up channel, while the negative one indicates that the spin-down channel dominates. $T_\uparrow$ and $T_\downarrow$ at the zero bias voltage through this FePc molecular junction is 4.6×10^{-4} and 0.26 G_0 (G_0 denotes the quantum constant and equals to e^2/h), respectively. It turns out that the calculated SFE at zero bias is about −99.8%, indicating that conductance through the molecular junction is mainly governed by the spin-down channel.

Now we turn to understand the diversity in the conductance of two spin channels according to the frontier molecular orbitals and magnetic moment (MM) analysis of the free FePc molecule. In FePc the D_{4h} crystalline field lifts the orbital degeneracy of the Fe 3*d* shell and splits the energy levels into a_{1g} (d_{z^2}), b_{2g} (d_{xy}), e_g (d_{xz},d_{yz}), and b_{1g} ($d_{x^2-y^2}$). The electronic configuration for the spin-up and spin-down electrons is $a_{1g}^1 b_{2g}^1 e_g^2$ and e_g^2, respectively. Consequently, the molecular MM is predicted to be 2.0 μ_B. The calculated results at the GGA-PBE level[35] show that the highest occupied molecular orbital (HOMO) of FePc molecule is determined to be a doubly degenerate MO with e_g symmetry, while the lowest unoccupied MO (LUMO) has b_{2g} symmetry. According to the Mulliken population, we find that the FePc molecular MM is mainly contributed by the Fe atom and its local atomic MM is 2.32 μ_B. Note that the nearest N atoms (the atomic MM is about −0.25 μ_B) connecting to the center Fe atom also give small contribution to the total MM, and antiferromagnetically couple to the Fe atom. In the two-probe system, the FePc molecular MM (about 2.18 μ_B) does not significantly change due to the presence of GNR electrodes, and the Fe atom (the atomic MM is about 2.45 μ_B) still antiferromagnetically couples to the neighboring N atoms. The significant transmission peak labeled with **A** in Fig. 3(a) is mainly contributed by the spin-down MO just below the HOMO (HOMO-1), which is delocalized over the whole molecular junction, as shown in Fig. 3(b). The low and sharp transmission (labeled with *) at −0.03 eV originates from the perturbed HOMO, which is mainly localized at the center region of FePc molecule and the Fe d_{xy} orbital gives its considerable contribution. As seen in Fig. 3(b), we can conclude that the narrow and sharp transmission peak labeled with **B** comes from the spin-down FePc-electrode hybrid state originated from the coupling between the electrode and Fe's d_{xy} and d_{z^2} atomic orbitals.

Next, to further explore the mechanism the NDR observed in the proposed FePc molecular junction with two N-doped 13-AGNRs, we plot the spin-polarized transmission spectra at the different bias voltages in Fig. 4. It is clear that the transmission curves gradually shift toward the low-energy side and their shapes change dramatically with the applied bias voltage, especially for the spin-down channel. For the spin-down electrons, when V_{bias} increases, the transmission peak **A** originated from the HOMO-1 becomes narrow gradually, accompanied by a change in heights. As a result, the current of spin-down electrons continuous increases and reaches its maximum value at V_{bias} = 0.14 V. When V_{bias} continuously increases to 0.5 V, the feature of the spin-down transmission function changes dramatically. The transmission peak **A** is strongly suppressed and even disappears, probably due to a change in its effective coupling to the N-doped AGNRs under the bias voltage.[36] As a result, in the energy range from −1.25 to 0.3 eV, the transmission coefficients of

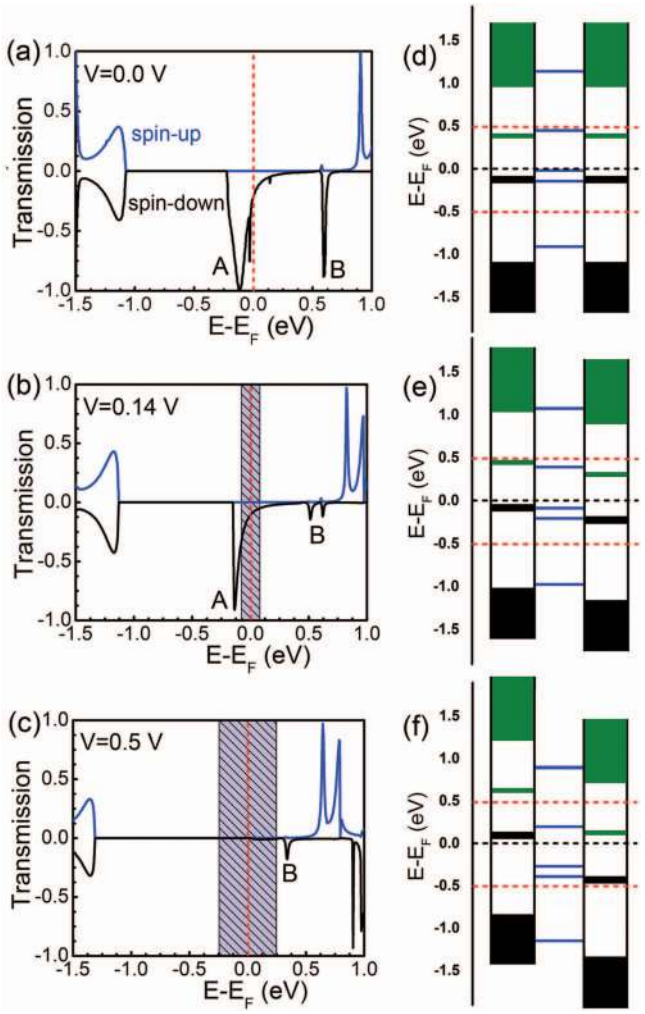

FIG. 4. The bias dependent transmission spectra of FePc molecular junction. (a) 0.0 V, (b) 0.14 V, and (c) 0.5 V. Here, the red vertical dotted line labels the Fermi level and the purple shadow area stands for the integral energy range under the applied bias. (d)–(f) Schematic illustration of the molecular projected self-consistent Hamiltonian eigenvalues in scattering region relative to these discrete bands in two N-doped armchair GNRs with bias voltages of 0.0, 0.14, and 0.5 V, respectively.

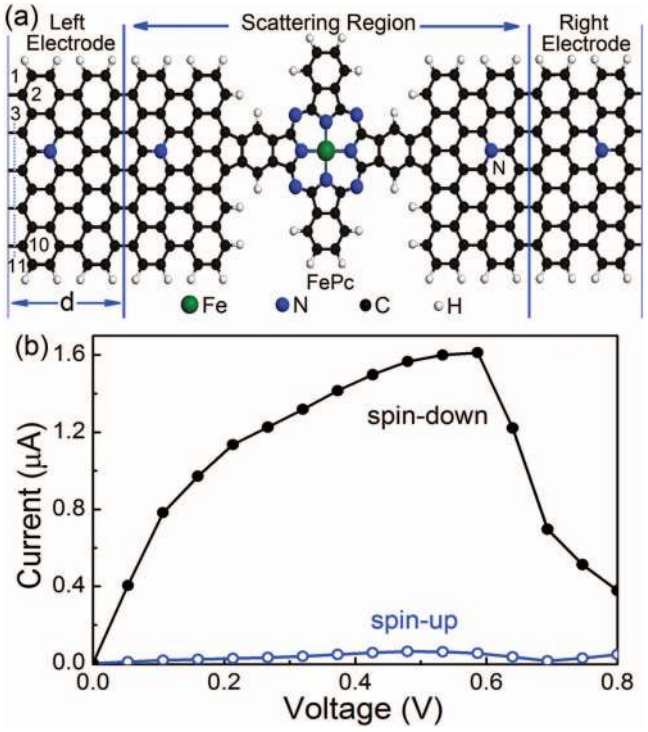

FIG. 5. (a) FePc molecular junction with N-doped 11-AGNR electrodes (W = 11). (b) The corresponding spin-resolved I-V curves.

the spin-down electrons are very small (less than 0.01). In our calculations, the electrons with inject energies in the interval [$-eV_{bias}/2$, $eV_{bias}/2$] (i.e., from -0.25 to 0.25 eV) can tunnel through the junction. Thus, the current decreases, and the I-V valley appears. When V_{bias} continually increases, the current increases again since the transmission peak **B** enters the integral energy window (i.e., $V_{bias} = 0.7$ V).

We also illustrate the origin of NDR with a schematic model presented in Figs. 4(d)–4(f). Here, two vertical bars stand for the density of states of the N-doped AGNRs, and five solid lines in between indicate the energy position of the discrete levels in the scattering region. For the junction with zero bias, the HOMO-1 in scattering region catches the upmost valence band of two N-doped AGNR leads, which results in the significant transmission peaks **A**. When V_{bias} increases to 0.14 V, the Fermi level shifts up and down by 0.07 eV for the left and right electrodes, respectively. The localized HOMO matches the upmost valence band of the left electrode, while the delocalized HOMO-1 touches the upmost valence band of the right electrode. Compared to the zero bias case, due to the relative worse matching, the transmission peak from the HOMO-1 is suppressed and becomes narrow and sharper, as shown in Fig. 4(b). When V_{bias} is 0.5 V, the HOMO-1 does not overlap effectively with the valence states of the left leads although it still touches the upmost valence state of the right electrode, which leads to negligible transmission coefficients for the spin-down electrons in the integral energy window. These observations suggest that the NDR appearing in the proposed molecular junction mainly originates from the bias-dependent effective coupling between the discrete frontier FePc molecular orbitals and the narrow density of states of N-doped AGNR electrodes.[26,27]

The N-doped 13-AGNRs are used in the proposed dual-functional FePc molecular junction. Here, we perform calculations of the FePc molecular junction with different AGNR widths (W = 11 and 12) to examine the size-dependent effect since the band gaps of AGNRs depend on its width and exhibit three distinct family (3n+m behavior).[37,38] As an example, the two-probe FePc molecular junction with N-doped 11-AGNR electrodes is illustrated in Fig. 5(a). Figure 5(b) shows the spin-polarized I-V curves of FePc molecule sandwiched between two N-doped 11-AGNRs in the bias voltage range from 0.0 to 0.8 V. Clearly, this examined molecular junction shows obvious spin transport polarization. The current of the spin-down electrons is larger than that of the spin-up electrons. The SFE is predicted to be about -99.0%. More importantly, the junction also displays obvious NDR. Although similar results are obtained for the FePc molecule sandwiched between two N-doped 12-AGNRs, we note that the value and position of the maximum currents of the spin-up and spin-down electrons depend on the width of AGNRs.

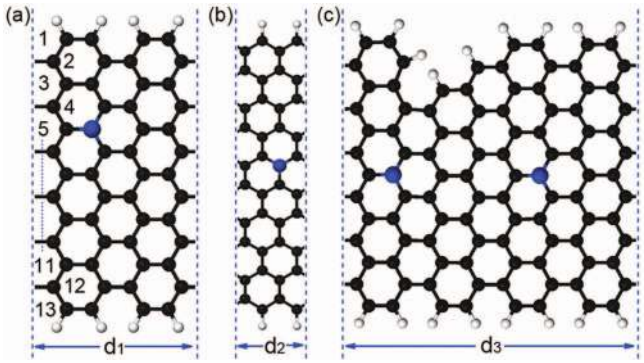

FIG. 6. Three examined GNR electrodes. (a) AGNR (W = 13, N dopant locates at the off-center site), (b) ZGNR (W = 10), (c) GNR with the mixed armchair and zigzag edges. Here, d_1, d_2, and d_3 are 8.53, 4.95, and 17.06 Å, respectively, which stand for the optimized lattice constant of three different N-doped GNR electrodes.

For example, the maximum current through FePc molecular junction with N-doped 11-AGNRs is 1.62 μA at about 0.6 V, while is different from the results shown in Fig. 2.

Since the edge shape of GNRs obtained in experiments is complex including both zigzag and armchair edges,[39–41] we also investigate the effect of the edge shape of GNRs on the transport properties of GNR-FePc-GNR junctions as well as the N doping site in AGNR electrodes. Here, we examine three FePc molecular junctions with different GNR electrodes. The corresponding GNR electrodes are shown in Fig. 6. The main results, including the spin-resolved transmission coefficients ($T_\uparrow$ and $T_\downarrow$), SFE at zero bias, and the currents of the spin-down electrons at two bias voltages ($I_\downarrow(V_1)$ and $I_\downarrow(V_2)$), are summarized in Table I. When the N atom dopes at different site in 13-AGNR electrodes, as shown in Fig. 6(a), the conductance through FePc molecular junction (MJ_1) is mainly governed by the spin-down channel and the high SFE is up to −99.9%. The current of the spin-down electrons ($I_\downarrow$) at 0.2 V and 0.5 is about 1.0 and 0.7 $\times 10^{-2}\mu$A, indicating that the obvious NDR appears in MJ_1. When an FePc molecule is sandwiched between two N-doped zigzag graphene nanoribbon (ZGNR) electrodes (MJ_2) (the electrode is shown in Fig. 6(b)), the $T_\uparrow$ and $T_\downarrow$ at the Fermi level is 1.5×10^{-3} and 8.5×10^{-2} G_0, respectively. It turns out that the SFE is about −96.5%. The obvious NDR is observed for MJ_2 since the $I_\downarrow$ at 0.2 V is larger than the $I_\downarrow$ at 0.4 V. Actually, the dual-function, namely, the high SFE and NDR, is still robust for the FePc molecule junction (MJ_3), where a FePc molecule connects to GNRs with the mixed armchair and zigzag edges. This kind of electrode is illustrated in Fig. 6(c). The SFE is about −99.8%. And the $I_\downarrow$ at 0.1 V is roughly 15 times larger than $I_\downarrow$ at 0.2 V.

TABLE I. The spin-resolved transmission coefficients ($T_\uparrow$ and $T_\downarrow$ in G_0), SFE (in %) at zero bias, and the currents of the spin-down electrons at two bias voltages ($I_\downarrow(V_1)$ and $I_\downarrow(V_2)$ in μA) for the FePc molecular junctions with three different GNR electrodes, as shown in Fig. 6.

Junctions	$T_\uparrow$	$T_\downarrow$	SFE	$I_\downarrow(V_1)$	$I_\downarrow(V_2)$
MJ_1	3.6×10^{-4}	8.3×10^{-1}	−99.9	1.00(0.2)	0.7×10^{-2}(0.5)
MJ_2	1.5×10^{-3}	8.5×10^{-2}	−96.5	0.68(0.2)	0.4×10^{-1}(0.4)
MJ_3	0.6×10^{-4}	7.1×10^{-2}	−99.8	0.15(0.1)	0.1×10^{-1}(0.2)

It should be pointed out that we consider the molecular junctions with suspended geometry. The substrate effect was not taken into account in our calculations. If the proposed molecular junctions adsorb on one substrate, the transport properties will be modulated by the subtle balance of couplings between the substrate/FePc molecular and the substrate/N-doped GNR electrode. Actually, it needs further investigations to explore the substrate effect.

IV. CONCLUSION

In summary, we design a dual-functional molecular junction by attaching FePc molecule to two N-doped GNR electrodes based on our spin-polarized first-principles calculations. The transmission spectra of the spin-up and spin-down electrons display remarkably different bias-dependent features. The zero-bias conductance through FePc molecule is dominated by the spin-down electrons. The observed NDR originates from the bias-dependent effective coupling between the discrete frontier FePc molecular orbitals in the scattering region and the density of states of N-doped AGNR electrodes. The dual-function, namely, high spin filter efficiency and NDR, is robust regardless of the edge shape, the width, and the N-doping site in GNRs. These mark the great promise of the FePc molecule junction for future molecular electronics and spintronics applications.

ACKNOWLEDGMENTS

This work is partially supported by the National Basic Research Program of China (No. 2011CB921404), by the National Natural Science Foundation of China (Nos. 20903003, 11074235, and 11034006), by the Knowledge Innovation Program of the Chinese Academy (No. KJCX2-YW-W22), by the Fundamental Research Funds for the Central Universities (No. WK2340000007), and Supercomputing Center of USTC, and by Shanghai Supercomputer Center. Work at NTU is supported in part by A*STAR SERC grant (No. M47070020) and MOE AcRF Tier-1 grant (No. M52070060).

[1] A. R. Rocha, V. M. García-suárez, S. W. Bailey, C. J. Lambert, J. Ferrer, and S. Sanvito, Nature Mater. **4**, 335 (2005).
[2] R. L. McCreery and A. J. Bergren, Adv. Mater. **21**, 4303 (2009).
[3] W. Y. Kim and K. S. Kim, Acc. Chem. Res. **43**, 111 (2010).
[4] S. Sanvito, Chem. Soc. Rev. **40**, 3336 (2011).
[5] A. D. Zhao, Q. X. Li, L. Chen, H. J. Xiang, W. H. Wang, S. Pan, B. Wang, X. D. Xiao, J. L. Yang, J. G. Hou, and Q. S. Zhu, Science **309**, 1542 (2005).
[6] C. Iacovita, M. V. Rastei, B. W. Heinrich, T. Brumme, J. Kortus, L. Limot, and J. P. Bucher, Phys. Rev. Lett. **101**, 116602 (2008).
[7] Z. Y. Li, B. Li, J. L. Yang, and J. G. Hou, Acc. Chem. Res. **43**, 954 (2010).
[8] X. Shen, L. Sun, E. Benassi, Z. Shen, X. Zhao, S. Sanvito, and S. M. Hou, J. Chem. Phys. **132**, 054703 (2010).
[9] X. Shen, L. L. Sun, Z. L. Yi, E. Benassi, R. X. Zhang, Z. Y. Shen, S. Sanvito, and S. M. Hou, Phys. Chem. Chem. Phys. **12**, 10805 (2010).
[10] S. B. Lopez, K. Park, V. García-Suárez, and J. Ferrer, Phys. Rev. Lett. **102**, 246801 (2009).
[11] M. Mannini, F. Pineider, P. Sainctavit, C. Danieli, E. Otero, C. Sciancalepore, A. M. Talarico, M. Arrio, A. Cornia, D. Gatteschi, and R. Sessoli, Nature Mater. **8**, 194 (2009).
[12] K. Xu, J. Huang, S. L. Lei, H. B. Su, F. Y. C. Boey, Q. X. Li, and J. L. Yang, J. Chem. Phys. **131**, 104704 (2009).

[13]J. Huang, Q. X. Li, K. Xu, H. B. Su, and J. L. Yang, J. Phys. Chem. C **114**, 11946 (2010).
[14]L. P. Zhou, S. W. Yang, M. F. Ng, M. B. Sullivan, V. B. C. Tan, and L. Shen, J. Am. Chem. Soc. **130**, 4023 (2008).
[15]X. Shen, Z. L. Yi, Z. Y. Shen, X. Y. Zhao, J. L. Wu, S. M. Hou, and S. Sanvito, Nanotechnology **20**, 385401 (2009).
[16]L. Wang, X. F. Gao, X. Yan, J. Zhou, Z. X. Gao, S. Nagase, S. Sanvito, Y. Maeda, T. Akasaka, W. N. Mei, and J. Lu, J. Phys. Chem. C **114**, 21893 (2010).
[17]Z. H. Cheng, L. Gao, Z. T. Deng, N. Jiang, Q. Liu, D. X. Shi, S. X. Du, H. M. Guo, and H.-J. Gao, J. Phys. Chem. C **111**, 9240 (2007).
[18]T. Tada, S. Hamayama, M. Kondo, and K. Yoshizawa, J. Phys. Chem. B **109**, 12443 (2005).
[19]A. Calzolari, A. Ferretti, and M. B. Nardelli, Nanotechnology **18**, 424013 (2007).
[20]K. S. Novoselov, A. K. Geim, S. V. Morozov, D. Jiang, Y. Zhang, S. V. Dubonos, I. V. Grigorieva, and A. A. Firsov, Science **306**, 666 (2004).
[21]A. K. Geim, and K. S. Novoselov, Nature Mater. **6**, 183 (2007).
[22]Z. Y. Li, H. Y. Qian, J. Wu, B. L. Gu, and W. H. Duan, Phys. Rev. Lett. **100**, 206802 (2008).
[23]X. L. Li, X. R. Wang, L. Zhang, S. Lee, and H. J. Dai, Science **319**, 1229 (2008).
[24]Y. D. He, H. L. Dong, T. Li, C. L. Wang, W. Shao, Y. J. Zhang, L. Jiang, and W. P. Hu, Appl. Phys. Lett. **97**, 133301 (2010).
[25]L. A. Agapito, and H. P. Cheng, J. Phys. Chem. C **111**, 14266 (2007).
[26]H. Cheraghchi and K. Esfarjani, Phys. Rev. B **78**, 085123 (2008).
[27]H. Ren, Q. X. Li, Y. Luo, and J. L. Yang, Appl. Phys. Lett. **94**, 173110 (2009).
[28]M. G. Zeng, L. Shen, Y. Q. Cai, Z. D. Sha, and Y. P. Feng, Appl. Phys. Lett. **96**, 042104 (2010).
[29]M. Koleini, M. Paulsson, and M. Brandbyge, Phys. Rev. Lett. **98**, 197202 (2007).
[30]J. M. Soler, E. Artacho, J. D. Gale, A. García, J. Junquera, P. Ordejón, and D. S. Portal, J. Phys.: Condens. Matter **14**, 2745 (2002).
[31]J. Perdew, K. Burke, and M. Ernzerhof, Phys. Rev. Lett. **77**, 3865 (1996).
[32]J. Taylor, H. Guo, and J. Wang, Phys. Rev. B **63**, 245407 (2001).
[33]M. Brandyge, J. L. Mozos, P. Ordejón, J. Taylor, and K. Stokbro, Phys. Rev. B **65**, 165401 (2002).
[34]J. Huang, Q. X. Li, H. Ren, H. B. Su, Q. W. Shi, and J. L. Yang, J. Chem. Phys. **127**, 094705 (2007).
[35]Since it has been argued that the hybrid functionals are more appropriate to deal with MPc molecules than GGA functionals, we also perform the hybrid functional calculations for the free FePc molecule. We find that the molecular magnetic moment and the spatial distribution of frontier molecular orbitals are not sensitive to the used functionals. The hybrid DFT calculations enhance the level spacings. The LUMO displays the B_{2g} symmetry and the HOMO with e_g symmetry is single occupied. When the FePc is attached to the N-doped AGNRs, the electronic configuration of FePc in the proposed junction becomes similar to that calculated with the hybrid functional.
[36]C. D. Pemmaraju, I. Rungger, and S. Sanvito, Phys. Rev. B **80**, 104422 (2009).
[37]Y.-W. Son, M. L. Cohen, and S. G. Louie, Phys. Rev. Lett. **97**, 216803 (2006).
[38]Z. F. Wang, Q. X. Li, H. X. Zheng, H. Ren, H. B. Su, Q. W. Shi, and J. Chen, Phys. Rev. B **75**, 113406 (2007).
[39]C. Tao, L. Jiao, O. V. Yazyev, Y.-C. Chen, J. Feng, X. Zhang, R. B. Capaz, J. M. Tour, A. Zettl, S. G. Louie, H. Dai, and M. F. Crommie, Nature Phys. **7**, 616 (2011).
[40]L. Sun, P. Wei, J. Wei, S. Sanvito, and S. M. Hou, J. Phys.: Condens. Matter **23**, 425301 (2011).
[41]O. V. Yazyev, R. B. Capaz, and S. G. Louie, Phys. Rev. B **84**, 115406 (2011).